PHYSICAL REVIEW B VOLUME 14, NUMBER 9 1 NOVEMBER 1976

Relating structural, magnetization, and hyperfine field studies to a local environment model in $Fe_{3-x}V_xSi$ and $Fe_{3-x}Mn_xSi$[†]

V. Niculescu, K. Raj,* J. I. Budnick, T. J. Burch, W. A. Hines, and A. H. Menotti
Department of Physics and Institute of Materials Science, The University of Connecticut, Storrs, Connecticut 06268

(Received 24 May 1976)

X-ray, magnetization, and spin-echo NMR techniques have been used to measure the changes in the atomic ordering along with the effect of these changes on the local moment and the internal field distributions in $Fe_{3-x}V_xSi$ alloys for $0 \leq x \leq 1.00$. We have shown that V continues to enter predominantly the *B* sites in the Fe_3Si matrix up to $x \approx 1.0$, which is the limit of V solubility. The $Fe_{3-x}V_xSi$ alloys are ferromagnetic up to $x \approx 0.9$ with the saturation magnetization decreasing linearly with x. V substitution into the *B* sites reduces the moments of the first-near-neighbor (1nn) Fe(*A*, *C*) atoms linearly from their initial value of $1.35\mu_B$ while the moments of Fe(*B*) atoms remain constant at $2.20\mu_B$. A model giving a detailed mechanism for the origin of the satellite structure observed in the NMR spectra is proposed for $Fe_{3-x}V_xSi$ as well as for $Fe_{3-x}Mn_xSi$, a previously measured system. According to this model, the changes in the transition-metal internal fields at *B* sites are produced as a result of changes in the 4*s* spin polarization induced by the perturbations of the 1nn Fe(*A*, *C*) moments. The values calculated from this model for the on-site hyperfine fields of Fe(*B*) and Mn(*B*) are -205 and -192 kOe, respectively. The on-site contribution to the V hyperfine field is estimated to be about 3 kOe with this model, in reasonable agreement with the very low moment value found for V. This detailed work suggests that the Fe(*A*, *C*) 1nn shell screens the *B* sites from any direct interaction with a more distant neighbor either magnetically or chemically. Using all of the NMR and magnetization data together with the model, a canting of the Mn moments in $Fe_{3-x}M_xSi$ for $0.75 < x < 1.6$ has been predicted. In addition, the disorder contributions to the NMR spectra have been identified.

I. INTRODUCTION

Since the first report[1] on the selective substitution of transition-metal impurities into the Fe_3Si matrix, a great deal of interest has been shown in this field.[2-11] This interest stems from the rather unique opportunities the system provides for understanding and correlating magnetic and structural properties and also of comprehending the influence of neighbor environments on hyperfine interactions. The last idea was the central theme of detailed NMR and x-ray work of Niculescu *et al.*[6,9] on the alloys $Fe_{3-x}Mn_xSi$ over a wide composition range $0 \leq x \leq 1.60$, where it was shown that changes in the magnetic structure and hyperfine fields are directly correlated with the degree of local atomic ordering. Furthermore, this system exhibits clear conduction-electron-polarization effects.

In order to extend our knowledge of the neighbor environment effects on the hyperfine interactions and magnetic behavior, we have made a detailed investigation of the structural and magnetic properties of the system $Fe_{3-x}V_xSi$ over the composition range $0 \leq x \leq 1.25$. This study enables us to (i) further explore the selectivity mechanism in the Fe_3Si matrix, (ii) investigate the correlation between the local atomic environment and the onset of the long-range magnetic order in this system, and (iii) evaluate the role of the conduction-electron polarization in the hyperfine-interaction picture.

The correlation between the structural, magnetization, and NMR results in both the $Fe_{3-x}Mn_xSi$ and $Fe_{3-x}V_xSi$ systems permits a quantitative evaluation of the local *s* spin polarization by 3*d* magnetic moments at neighboring atoms. Thus a consistent picture of the moment and hyperfine-field perturbation functions of the near-neighbor (nn) configurations and the nature of the substituted atoms is derived.

The structural data on the $Fe_{3-x}V_xSi$ alloys are obtained to determine the limit of solubility and the effect on the atomic ordering. The magnetic and hyperfine-field behavior of the $Fe_{3-x}V_xSi$ alloys can be successfully analyzed using a model in which the Fe magnetic moments are critically dependent on the number of Fe atoms in the first-near-neighbor (1nn) shell regardless of their magnetic moments. According to this model it will be shown that the substitution of the impurities Mn and V in a distant-neighbor shell perturbs the moment and hyperfine field on a specific atom through the changes in its 1nn. A detailed discussion of the correlation between the nature of the substituted atom, its moment and local spin polarization effects in the near-neighbor shells is also presented.

II. $Fe_{3-x}V_xSi$ SYSTEM

The intermetallic compound Fe_3Si is a well-ordered ferromagnet. Its crystal structure, the face-centered-cubic DO_3 type, is shown in Fig. 1. The structure exhibits four crystal sites A, B, C, and D, with the specific neighbor configurations summarized in Table I. Notations used to indicate occupancy of a site with an element is as follows: Fe in the B site is represented by Fe(B), Si in the D site by Si(D), etc.

The Fe atoms are located in three crystal sites, A, B, and C with A and C being chemically and magnetically equivalent. The Fe(A,C) have four Fe(B) and four Si(D) as 1nn and carry a magnetic moment of $1.35\mu_B$ while the Fe(B) have eight Fe 1nn and carry a magnetic moment of $2.20\mu_B$.[10,12] The measured hyperfine fields at 1.4 K are 218(2) kOe and 338(2) kOe for the Fe(A,C) and Fe(B) sites, respectively.[13,14] The Si(D) atoms have a small negative moment of $-0.07(06)\mu_B$ and a transferred hyperfine field of 37 kOe.

As originally shown by the NMR work of Burch *et al.*[1] and Litrenta,[2] and subsequently confirmed by the neutron-diffraction work of Pickart *et al.*,[3] small amounts of V substitute for Fe(B) in Fe_3Si. The ^{51}V hyperfine field in Fe_3Si has been found to be 47.7 kOe,[1] while the magnetization studies of Hines *et al.*[10] suggest that a zero local magnetic moment is associated with the V impurities. The x-ray studies of Bergner *et al.*[15] indicated that V forms a solid solution in $Fe_{3-x}V_xSi$ between $x=0$ and 0.7 preserving the cubic DO_3-type crystal structure, with a slight increase in the lattice constant and a depression of Curie temperature as the V concentration increases.

III. EXPERIMENTAL

A. Sample preparation

Pure Fe(99.999%), V(99.95%), and Si(99.99%) in appropriate proportions were used to make 10-g ingots for each of the $Fe_{3-x}V_xSi$ alloys with the following compositions: $x=0$, 0.01, 0.02, 0.04, 0.08, 0.15, 0.25, 0.50, 0.75, 0.90, 1.0, and 1.25. An off-stoichiometric composition of $Fe_{3.04}V_{0.04}Si_{0.92}$ was also made.

The elements were mixed and melted several times in an argon arc furnace to ensure homogeneity. The weight loss after arc melting was less than 1% for all the alloys. After arc melting each ingot was sealed under vacuum (2×10^{-6} Torr) in a quartz tube and homogenized for 40 h at 800 °C. The temperature was then decreased slowly to 600 °C over a period of five hours and was subsequently quenched from 600 °C into room-temperature water. The homogenized ingots were powdered to No. 325 mesh size and annealed at

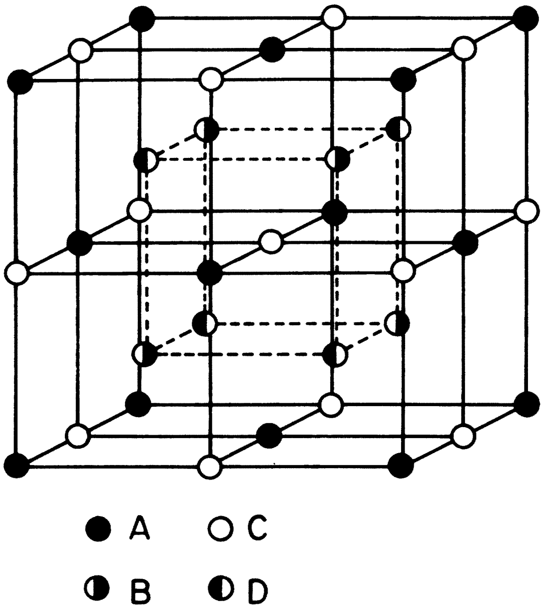

FIG. 1. Unit cell of $Fe_{3-x}V_xSi$ alloys. The sites are represented by A, B, C, and D. The A and C sites are equivalent and are occupied by Fe atoms, the B site is occupied by Fe and V, and the D site by Si.

TABLE I. Fe_3Si neighbor configurations.

No. of shell	1	2	3	4	5	6	7	8
Neighbor distance in lattice parameters	0.43	0.5	0.705	0.83	0.86	1	1.08	1.11
A,C	4B 4D	6A,C	12A,C	12B 12D	8A,C	6A,C	12B 12D	24A,C
B	8A,C	6D	12B	24A,C	8D	6B	24A,C	24D
D	8A,C	6B	12D	24A,C	8B	6D	24A,C	24B

600 °C for 1 h under vacuum (2×10^{-6} Torr). The samples were slowly cooled to room temperature within the furnace.

These powders were used for the structural, magnetization and NMR studies reported below. The x-ray analysis of the samples showed that for $x<1$ the alloys were single phase and for $x\geq 1$ additional phases were observed.

B. Structural properties

The x-ray measurements were performed at room temperature using a Philips diffractometer and Cu $K\alpha$ radiation. Up to $x=1$, the samples were single phase and the x-ray diffraction patterns could be indexed on a fcc structure. The lattice parameters were obtained by extrapolation to $\theta=90°$ for the parameters corresponding to reflections from the (440), (620), and (444) planes for both $K\alpha_1$ and $K\alpha_2$ radiations. At $x=1$, a small amount of a second phase (<1%) was found. The amount of the additional phase increased with x. In Table II, a summary of our x-ray data is presented. It can be seen that the substitution of V in Fe_3Si, increases the lattice parameter up to 0.3% at the limit of solubility.

As shown in Fig. 1, the unit cell is composed of four interpenetrating fcc sublattices A, B, C, and D with origins situated at $A(0,0,0)$, $B(\frac{1}{4},\frac{1}{4},\frac{1}{4})$, $C(\frac{1}{2},\frac{1}{2},\frac{1}{2})$, and $D(\frac{3}{4},\frac{3}{4},\frac{3}{4})$. In this structure, Bragg reflections are produced by either all even or all odd Miller indices with the following three structure amplitudes:

$$\begin{aligned} &F_1 \sim [(f_A-f_C)^2+(f_B-f_D)^2]^{1/2} && \text{for } h,k,l \text{ all odd}, \\ &F_2 \sim f_A-f_B+f_C-f_D && \text{for } \tfrac{1}{2}(h+k+l)=2n+1, \\ &F_3 \sim f_A+f_B+f_C+f_D && \text{for } \tfrac{1}{2}(h+k+l)=2n, \end{aligned} \tag{1}$$

where f_A, f_B, f_C, f_D are average scattering factors for the atoms on A, B, C, and D sites, respectively, and n is an integer. The reflections for which $\frac{1}{2}(h+k+l)=2n$ are fundamental and are unaffected by the state of chemical order while the reflections with h,k,l all odd or all even with $(h+k+l)=2(2n+1)$ are superlattice reflections and their intensities depend upon the state of order.

When a random disorder occurs in ternary alloys of this type, all the superlattice lines are reduced in intensity by a factor S^2, where S is the long-range-order parameter and can be defined as in binary alloys by

$$S=(N-N_r)/(N_0-N_r),$$

where N is the number of atoms located on their ordered sites, N_0 those in the fully ordered state, and N_r in the randomly ordered state. However, if preferential disorder occurs between certain sites, then the two groups of superlattice reflections will be affected differently, and generally it is necessary to have more than one ordering parameter for the characterization of the state of order. Johnston and Hall[16] and Webster[17] discussed the effects of different types of disorder on the structure amplitudes of ternary alloys of the Heusler $L2_1$ type by introducing a parameter which describes the $B \leftrightarrow D$ disorder.

For Fe_3Si in a perfectly ordered state, $f_A=f_B=f_C$ so that the ratio of the intensities superlattice lines $F_{111}^2/F_{200}^2=1$. Measurements on a carefully prepared Fe_3Si sample by the method described above, showed essentially no disorder between Fe and Si sites. In the $Fe_{3-x}V_xSi$ system, previous NMR investigations[1,2] showed that V impurities replaces Fe in B sites. In general the disordering can then occur between $B\leftrightarrow D$, $(A,C)\leftrightarrow D$, and $(A,C)\leftrightarrow B$ sites.

Since V($Z=23$) and Fe($Z=26$) are very close to each other in the Periodic Table, their x-ray scattering factors are similar and thus disorder between B and (A,C) sites is difficult to distinguish by x-ray studies. However, the $B\leftrightarrow D$ and $(A,C)\leftrightarrow D$ disorder can be described by introducing the parameters α and β as fractions of (B) and (A,C) atoms which occupy the Si(D) sites. The ratio of the superlattice lines becomes

TABLE II. Structural parameters for the $Fe_{3-x}V_xSi$ system obtained from x-ray data. The values of the lattice parameters obtained by Bergner *et al.* (Ref. 15) are shown in the parentheses. We have assumed the $(A,C)\leftrightarrow B$ disorder to be zero. See note added in proof.

Alloy	Lattice constant (Å)	Calculated degree of disorder (%) $B\leftrightarrow D$ (α)	 $(A,C)\leftrightarrow D$ (β)
Fe_3Si	5.653 (5.650)	0	0
$Fe_{2.85}V_{0.15}Si$	5.6538	5	4
$Fe_{2.75}V_{0.25}Si$	5.654	8	4
$Fe_{2.5}V_{0.5}Si$	5.657 (5.661)	10	0
$Fe_{2.25}V_{0.75}Si$	5.6664	15	0
$Fe_{2.1}V_{0.9}Si$	5.668	10	0
Fe_2VSi	5.670	17	0

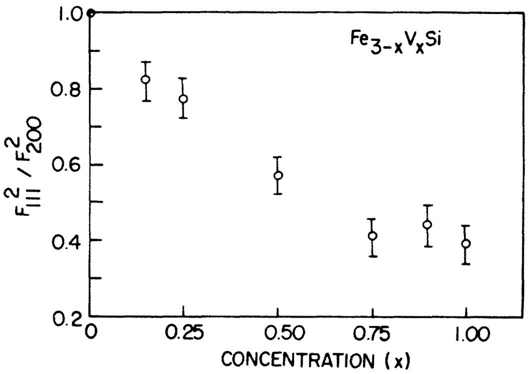

FIG. 2. Ratio of the superlattice structure factors F^2_{111}/F^2_{200} as a function of V concentration x in $Fe_{3-x}V_xSi$.

$$F^2_{111}/F^2_{200}=(1-2\alpha-\beta)^2/(1-2\beta)^2. \qquad (2)$$

The relative intensities of the superlattice lines have been normalized to the (444) fundamental line in the whole range of concentrations $0 \leq x \leq 1$. In the Fig. 2 we show the concentration dependence of the measured ratio F^2_{111}/F^2_{200} and in Table II, the values for the calculated parameters α and β are given. If the $(A,C) \leftrightarrow B$ disorder were to remain small, these data suggest an increase in $B \leftrightarrow D$ disorder with increasing V concentration. The $(A,C) \leftrightarrow D$ disorder on the other hand does not change significantly with the changes in alloy composition.

Because of the limitations of x-ray diffraction, one cannot exclude the possibility of $(A,C) \leftrightarrow B$ disorder. In order to have a more detailed picture of the site occupancy in the whole range of concentrations $0<x<1$ neutron-diffraction measurements are in progress. (See note added in proof.)

C. Magnetization results

The magnetic measurements were carried out over a temperature range from 3.0 to 1000 K and for magnetic fields up to 20 kOe by utilizing a P.A.R. Model 155 vibrating sample magnetometer (Foner method[18]) with the related cryogenic and oven accessories. The magnetometer was calibrated against the known saturation magnetization for nickel (room-temperature value 55.01 emu/g) while the low-temperature calibration was based on the ideal Curie-Weiss behavior of the paramagnetic salt $Gd_2(SO_4)_38H_2O$. The high-temperature calibration was based on the Curie-Weiss behavior for Gd_2O_3 and the known Curie temperature for nickel (631 K).

The measured bulk magnetizations (σ) versus applied magnetic field (H) for the samples with $0 \leq x \leq 0.75$ at 3 K saturate in a manner characteristic of ferromagnetism. In Fig. 3 the saturation magnetization extrapolated to 0 K and infinite field (σ_0) are plotted against V concentration.

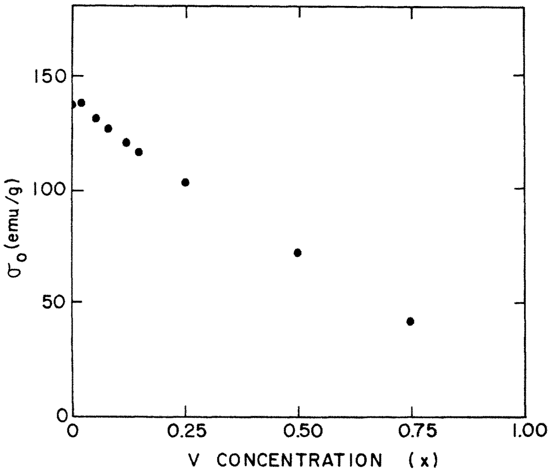

FIG. 3. Saturation magnetization (σ_0) (in emu/g) vs V concentration (x) for $Fe_{3-x}V_xSi$.

Figure 4 illustrates the behavior of ferromagnetic ordering temperature (T_C) as a function of the V composition. Also given are the values of the ordering temperature for $x=0.0$, 0.25, and 0.5 reported by Bergner *et al.*[15] Our measured Curie temperature for pure ordered Fe_3Si is 839(8) K. This value is in good agreement with two quite recent determinations [850 K (Ref. 19), 803 K (Ref. 20)] as well as several older measurements.[14] It is expected that the Curie temperature will be sensitive to stoichiometry and degree of order. We note that the Curie temperature values were reproducible for all $Fe_{3-x}V_xSi$ samples and,

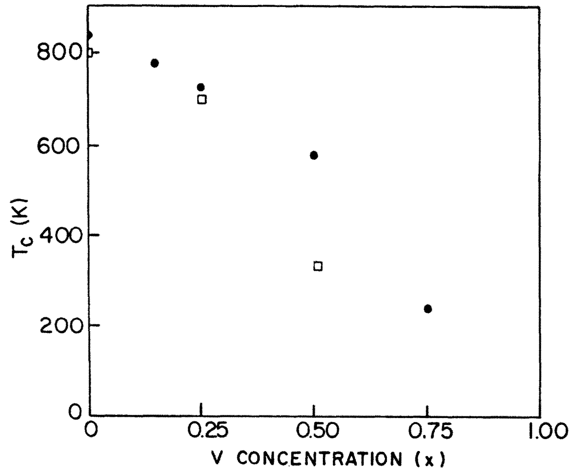

FIG. 4. Magnetic transition temperature (T_c) (in K) vs V concentration (x) for $Fe_{3-x}V_xSi$ (●). Also plotted are the values reported in Ref. 15 (□).

in addition, a duplicate sample of Fe_3Si gave the same Curie temperature (839 K) within experimental error.

In determining the ordering temperature for the $x = 0.75$ sample, measurements of the bulk magnetic moment versus temperature were made at various fields. The results, illustrated in Fig. 5, indicate a transition from the ferromagnetic to paramagnetic state at 240 K.

The measured bulk magnetizations versus magnetic field for $x = 0.75$, 0.90, and 1.00 samples at room temperature show typical paramagnetic behavior. For the $x = 0.90$ and 1.00 samples, measurements of the magnetization versus field were made at several temperatures. For these two samples, the dependence of σ is approximately linear at high fields and can be represented by the form

$$\sigma(H, T) = \chi(T) H + \sigma_0(T), \qquad (3)$$

where $\chi(T)$ is obtained from the slope and represents a susceptibility while $\sigma_0(T)$ is the intercept with the σ axis. The values of $\chi(T)$ and $\sigma_0(T)$ for the $x = 0.90$ and 1.00 samples are listed in Table III. Measurements of the bulk magnetic moment versus temperature for various fields were made for these samples. The typical high- and low-field behavior is shown for the $x = 0.90$ sample in Fig. 6 and the $x = 1.00$ sample in Fig. 7. A possible magnetic transition at about 15 K is indicated for the $x = 0.90$ composition while no such transition was observed above 3 K for the $x = 1.00$ sample.

D. Hyperfine-field distributions

The hyperfine-field measurements on the $Fe_{3-x}V_xSi$ alloys ($0 \le x \le 1.00$) were made at 1.3 K and in zero external magnetic field. A spin-echo NMR technique, fully described elsewhere,[22] was used. The echo amplitude was divided by frequency (ν), correcting only for the frequency variation of the Boltzmann distribution.

Spin echoes for all three nuclei in the $Fe_{3-x}V_xSi$ alloys are observed in the frequency range 14–60 MHz. For low V concentrations ($x \le 0.04$) all three signals Fe, V, and Si appear in this frequency region and are clearly resolved. Figure 8 shows the NMR spectra for alloys with $x = 0.02$ and 0.04 compared to that of Fe_3Si, for which the assignment of the lines is well known.[14]

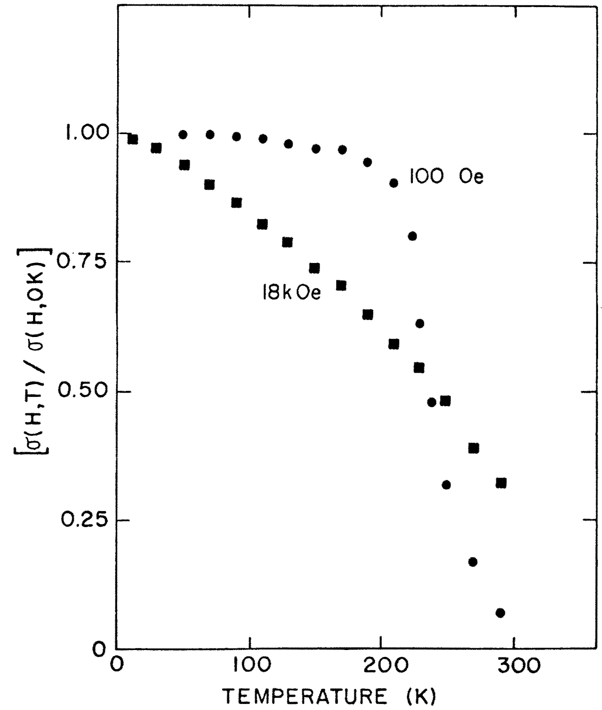

FIG. 5. Normalized magnetization $[\sigma(H, T)/\sigma(H, 0\text{K})]$ vs temperature, for $Fe_{2.25}V_{0.75}Si$ for the external magnetic fields $H = 100$ Oe (●) and $H = 18$ kOe (■). The magnetization at 0 K corresponding to these fields are $\sigma(100\text{ Oe}, 0\text{ K}) = 3.72$ emu/g and $\sigma(18\text{ kOe}, 0\text{ K}) = 41.9$ emu/g.

The main resonance of ^{51}V nuclei in the sample $Fe_{2.98}V_{0.02}Si$ is observed at 53.0 MHz compared to its value of 98.5 MHz reported in dilute Fe-V alloys.[23] Since the isotopic abundance and the relative detection sensitivity at constant frequency for ^{51}V (100% and 5.52) are much larger than ^{57}Fe

TABLE III. Values of $\chi(T)$ and $\sigma_0(T)$ obtained from the field dependence of the magnetization σ at different temperatures for the samples $Fe_{2.1}V_{0.9}Si$ and Fe_2VSi.

Sample	T (K)	$\chi(T)$ (10^{-6} emu/g)	$\sigma_0(T)$ (10^{-2} emu/g)
$Fe_{2.1}V_{0.9}Si$	3.3	270(5)	820(5)
	10.3	270(5)	810(5)
	48.2	270(5)	675(5)
	295	69(5)	450(5)
Fe_2VSi	3.7	51.8(5)	24.8(5)
	44.2	46.6(5)	13.5(5)
	295	15.6(5)	10.7(5)

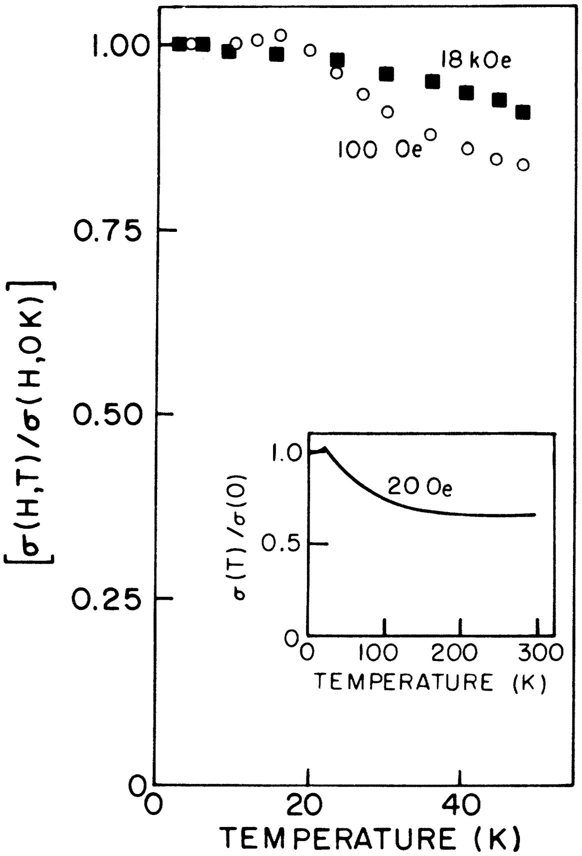

FIG. 6. Normalized magnetization [$\sigma(H,T)/\sigma(H,0\ \mathrm{K})$] vs temperature T (in K), for $\mathrm{Fe_{2.10}V_{0.90}Si}$ in two external fields $H=100$ Oe (○) and $H=18$ kOe (■). The magnetization at 0 K corresponding to these fields are: σ(100 Oe, 0 K) = 0.195 emu/g and σ(18 kOe, 0 K) = 14.5 emu/g. [Insert shows $\sigma(H,T)/\sigma(H,0\ \mathrm{K})$ for $H=20$ Oe.]

(2.2% and 0.03) and ^{29}Si (4.7% and 9.2), V completely dominates the spectrum at higher values of x. In the $x=0.02$ sample, the total integrated intensity of V NMR is about 40 times larger than the combined intensities of Fe(B), Fe(A,C), and Si(D) resonances. For higher x, this difference is even larger. In Fig. 9 the spectra of $x=0.15$, 0.25, 0.50, 0.75, and 0.9 are shown.

The V(B) and Fe(B) internal field distributions in $\mathrm{Fe_{3-x}V_xSi}$ bear strong resemblance with the Mn(B) and Fe(B) in $\mathrm{Fe_{3-x}Mn_xSi}$.[9] The V(B) and Fe(B) satellite structures arise from impurity substitution in the 3nn shell. The peaks labeled 0,1,2, etc., in the ^{51}V spectrum indicate the internal field at V(B) with 0,1,2, etc., V impurities in the 3nn shell, respectively. Similar explanation holds for the structure of the Fe(B) resonance and the same system is used for labeling the spectrum. The structure observed on the Si(D) line is due to V entering the 2nn shell (see Table I). A detailed

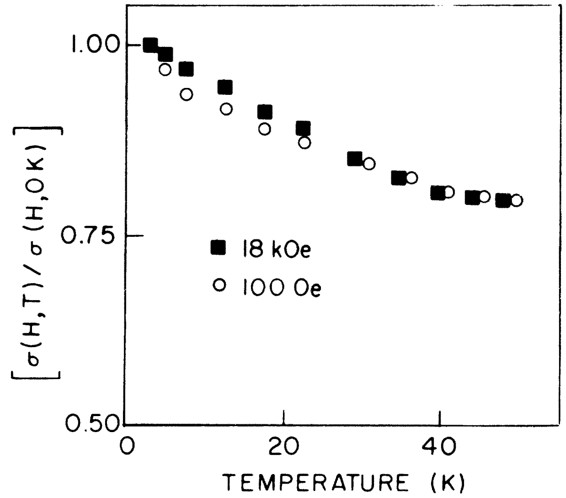

FIG. 7. Normalized magnetization [$\sigma(H,T)/\sigma(H,0\ \mathrm{K})$] vs temperature T (in K), for $\mathrm{Fe_2VSi}$ in two external magnetic fields $H=100$ Oe (○) and $H=18$ kOe (■). The magnetization at 0 K corresponding to these fields are σ(100 Oe, 0 K) = 1.5×10^{-2} emu/g and σ(18 kOe, 0 K) = 1.20 emu/g.

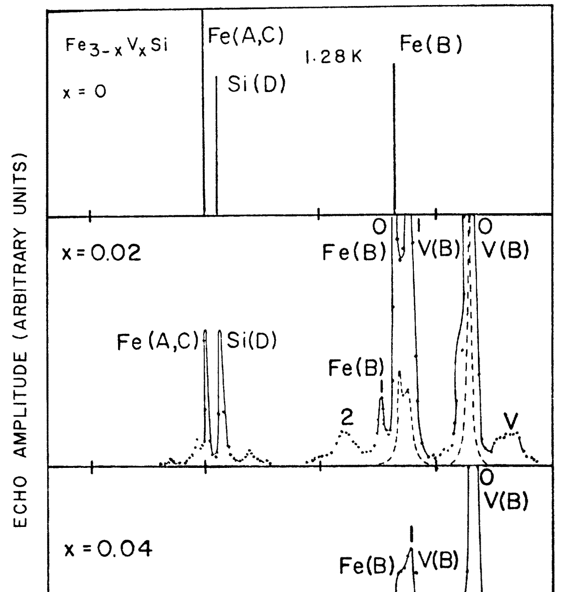

FIG. 8. Spin-echo spectra of $\mathrm{Fe_{3-x}V_xSi}$ alloys for $x=0$, 0.02, and 0.04, at 1.3 K. The assignments of different lines to specific nuclei are shown (also see the text). The line intensities are in arbitrary units and the spectra are drawn to show low intensity details. The dashed line inserts at about 46, 48, and 53 MHz for $x=0.02$ spectrum show the relative intensity of the Fe(B_0), V(B_1), and V(B_0) lines.

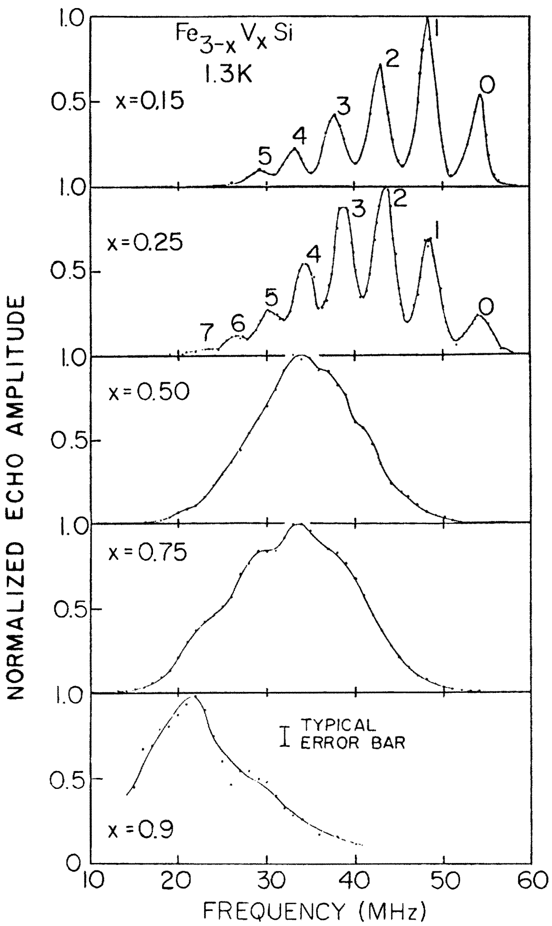

FIG. 9. Spin-echo spectra of Fe$_{3-x}$V$_x$Si for $x = 0.15$, 0.25, 0.5, 0.75, and 0.9 at 1.3 K. The spectra are dominated by ^{51}V resonance and no resolved lines due to Fe and Si nuclei are observed.

discussion of the satellite structure and the mechanism involved will be given in Sec. IV. For V concentrations exceeding $x = 0.25$ the satellite structure is not resolved (Fig. 9). With increasing V concentration, the resonance line shifts to lower frequencies and the power needed to excite the signal increases sharply indicating a loss of enhancement. For $x = 1$, a very weak signal has been observed at ~14 MHz.

IV. DISCUSSION

A. Background for the model

The analysis of the experimental results presented in Sec. III will be made using a model which describes the dependence of the magnetic moment for Fe(A,C) on the number of Fe atoms in the first near neighbor shell (see Fig. 10). As the discussion unfolds, it will be shown that this description for the Fe(A,C) moments provides an excellent fit for all of the NMR and magnetization data. The formulation of the model has resulted from a consideration of the hyperfine field[13,14] and magnetization[4,10] behavior of a series of binary Fe$_{1-c}$Si$_c$ alloys and the magnetization[10] behavior of a series of ternary Fe$_{3-x}$V$_x$Si alloys.

Mössbauer and NMR investigations of the ^{57}Fe nuclei in the Fe$_{1-c}$Si$_c$ system have yielded information concerning the hyperfine field at the various Fe sites.[13,14] In particular, these investigations have shown that the hyperfine field at the Fe(A,C) sites is strongly dependent on the number of Fe 1nn. Recent bulk magnetization work on a series of binary Fe-Si alloys in which the composition was varied about the Fe$_3$Si stoichiometry has demonstrated that the Fe(A,C) moment scales with the hyperfine field.[10] The measured saturation magnetization for Fe$_3$Si was found to be $\sigma = 137.8$ emu/g which is consistent with effective moment assignments of $+2.20\mu_B$, $+1.35\mu_B$, and $-0.07\mu_B$ for Fe(B), Fe(A,C), and Si, respectively. These values are in agreement with the moments obtained directly from polarized-neutron experiments.[12] Furthermore it was noted[10] that Fe(B) resembles bcc Fe in that both are surrounded by eight Fe 1nn and carry about the same moment of $+2.20\mu_B$. It was also noted that the ratio of the moments $\mu[\mathrm{Fe}(A,C)]/\mu[\mathrm{Fe}(B)]$ for Fe$_3$Si is $(+1.35\mu_B/+2.20\mu_B) = 0.61$ which compares well with the ratio of the hyperfine fields for sites with four Fe 1nn to those with eight Fe 1nn ($= 0.64$). The magnetization data for the binary Fe-Si alloys were described quite well by a model based on a substitution between the Fe(B) and Si(D) sites using the above moment assignments (i.e., excess Fe with a moment of $+2.20\mu_B$ replaces Si with a moment of $-0.07\mu_B$ and vice versa) and a scaling of the Fe(A,C) moments with the corresponding hyperfine fields.

Figure 10 summarizes the model describing the relative Fe(A,C) moment as a function of the number of Fe atoms in its 1nn shell. The open circles are the actual values of the magnetic moments calculated by scaling for atoms having six to three Fe 1nn. For less than three Fe 1nn the curve is extended by a simple extrapolation. One should notice that it goes through 0 for zero Fe 1nn.

In describing the saturation magnetization, σ_0, for the Fe$_{3-x}$V$_x$Si alloys with $x \leq 0.75$, we employ the above model. According to the preferential site selection, V replaces Fe in the B sites when forming Fe$_{3-x}$V$_x$Si. We assign V a moment of zero and, in addition, consider the influence of the substituted V on the Fe(A,C) moments only.[10] This is reasonable since V is in the 1nn shell for Fe(A,C) while only as close as the 3nn shell for Fe(B). Consequently, by employing Fig. 10 for the ternary

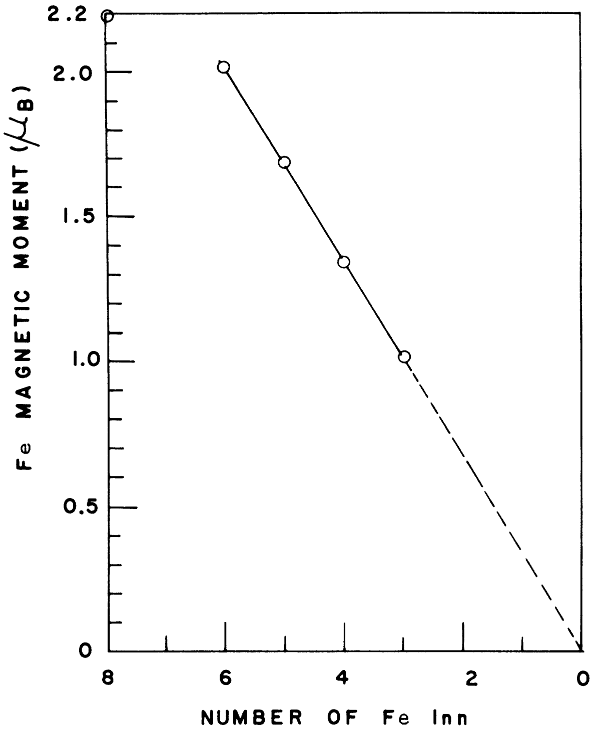

FIG. 10. Magnetic moment at the Fe(A,C) sites (in μ_B) versus the number of Fe 1nn for the binary Fe-Si system. The moment for 8 Fe 1nn is $2.2\mu_B$. The solid line and closed symbols are taken by scaling the Fe moments with the corresponding hyperfine fields and the dashed line is a linear extrapolation.

$Fe_{3-x}V_xSi$ system, we are assuming that in determining the Fe(A,C) moment, the replacement of an Fe(B) atom by a V atom is equivalent to replacing an Fe(B) atom by a Si atom, i.e., the Fe(A,C) moment has the *same* dependence on the number of 1nn Fe atoms that existed in the binary $Fe_{1-c}Si_c$ system. In $Fe_{3-x}V_xSi$ alloys, Fe(A,C) has four or less Fe 1nn since some of the Fe(B) are replaced by V. The saturation magnetization for $Fe_{3-x}V_xSi$ expressed in number of Bohr magnetons per formula unit, can be written

$$\sigma_0=(1-x)(+2.20)+x[\mu(\mathrm{V})]+(-0.07)+2\sum_{i=0}^{4}P_i\mu_i, \quad (4)$$

where $\mu(\mathrm{V})$ is the moment in Bohr magnetons on the substituted V (approximately zero), μ_i is the moment of an Fe(A,C) atom with i 1nn of Fe(B) (taken from Fig. 10), and P_i is the probability of an Fe(A,C) atom having i 1nn of Fe(B). In general, for a dilute random alloy with a fractional impurity concentration, x, the probability of finding m impurities in any nearest neighbor shell of n sites can be calculated from

$$P_n(m)=[n!/m!(n-m)!]x^m(1-x)^{n-m}. \quad (5)$$

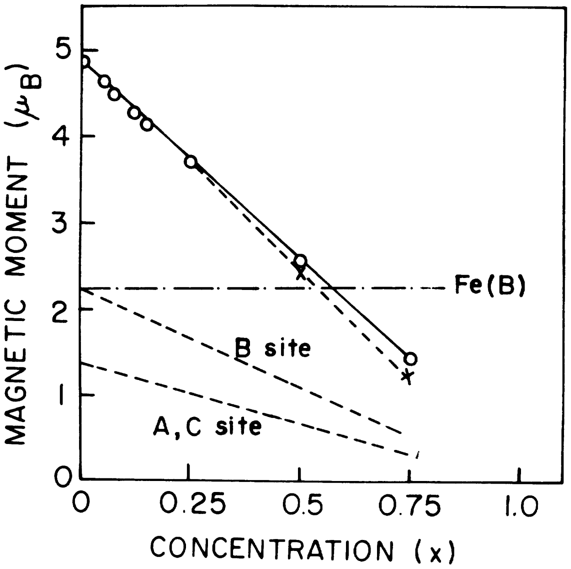

FIG. 11. Experimental bulk magnetization (in μ_B per formula unit) for $Fe_{3-x}V_xSi$ alloys in the composition range $0<x<0.75$. The experimental results are shown by solid line and open circles and the calculated values using the model described in Fig. 10 by the dashed line and crosses. The calculated average moments per B and (A,C) sites are also shown.

The P_i values for Eq. (4) can be easily calculated by a suitable application of Eq. (5). In Fig. 11, the measured values of the magnetic moment per formula unit are indicated (solid curve) along with the values calculated from Eq. (4) (dashed curve). It can be seen that at low concentration the calculated values are in perfect agreement with the experimental data. At high concentrations one can notice slightly lower values of the calculated moments. The over-all agreement between the measured magnetization and that obtained by using the model is indeed quite good. In Fig. 11 are also shown the values of the average magnetic moment per site in the concentration range $0<x<0.75$. It can be seen that μ[Fe(A,C)] decreases from $1.35\mu_B$ for Fe_3Si to ~$0.35\mu_B$ for $x=0.75$, while μ[Fe(B)] has a constant value, the decrease in the average moment per B site is the effect of a simple dilution of the B sublattice with V.

In $Fe_{3-x}Mn_xSi$, a similar system, neutron-diffraction measurements have shown that Mn occupies the B sites with a moment close to $2.2\mu_B$ and produces a decrease in the average moment per Fe(A,C) site from 1.35 at $x=0$ to $0.4\mu_B$ for $x=0.75$, while the Fe(B) moments remain unchanged with the Mn substitution (Fig. 12). This decrease has roughly the same behavior as that calculated for the V alloys. It seems that the decrease in Fe(A,C) magnetic moment due to the

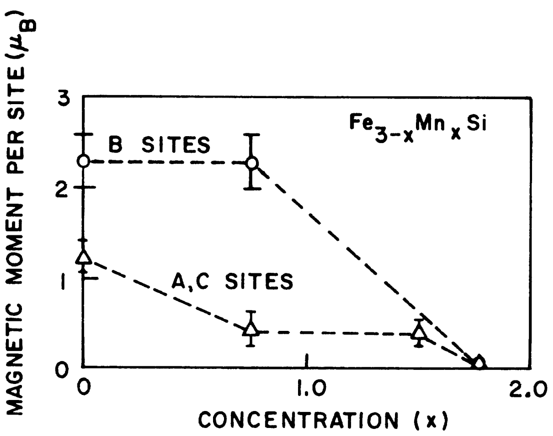

FIG. 12. Variation of (A, C) and B sites magnetic moment as a function of concentration (x) in $Fe_{3-x}Mn_xSi$ alloys. The data are those of Yoon *et al*. (Ref. 19). We have assumed a linear extrapolation between the data points.

presence of Mn or V in the first nn shell (see Table I) is independent of whether the substituted atom carries a magnetic moment or not.

B. Model for the V hyperfine-field contributions

For transition metals, the internal field at a particular nucleus is assumed to arise from (i) a core polarization H_{cp} due to the exchange interaction between $3d$ electrons and the inner s-like shells; (ii) a $4s$-like spin polarization contribution due to self polarization of the s-like electrons by the atom itself H_s; and (iii) the over-all spin-polarization (SP) effects from all the neighbors H_{sp}

$$H_{int} = H_{cp} + H_s + H_{sp}. \tag{6}$$

The effect of the presence of an impurity in the matrix can be described by a simple phenomenological model where the change in the field at a given host site near the impurity is due to a change in the local d moment on the host site and a change in the transferred $4s$ spin polarization field on the host site due to moment changes in the near-neighbor shells. The same model can be applied for the impurity hyperfine field.

Since V atoms have a negligible moment, the only effective mechanism for the hyperfine field on a V nucleus becomes the $4s$ spin polarization due to the neighboring moments. Therefore we can write

$$H_{int}(V) = H_{sp}. \tag{7}$$

In the first approximation, if we take into account the SP effects extending to the first three near-neighbor shells, the internal field is the sum

$$H_{int}(V) = H_{sp}[Fe(A, C)]_{1nn} + H_{sp}[Fe(B)]_{3nn}. \tag{8}$$

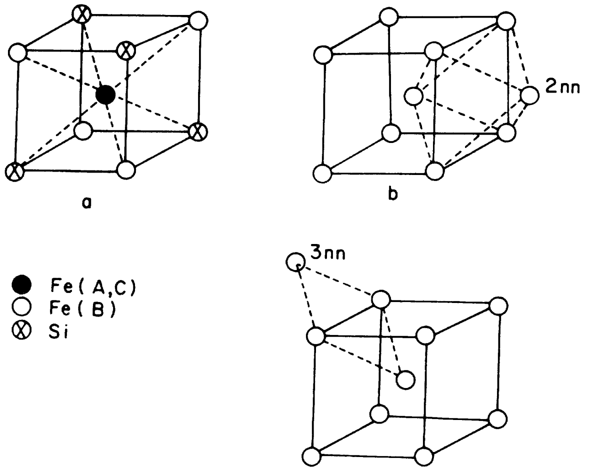

FIG. 13. Different configurations used in calculation of the moment perturbation due to impurity substitutions in the first- second- and third-nn shells around a specific atom. The dotted lines connect the first-nn atoms.

As shown before, a V impurity replacing Fe(B) in Fe_3Si produces a moment perturbation in the first-near-neighbor Fe(A, C) shell, while Fe(B) moments in the third-near-neighbor shell remain unchanged. Our model predicts a linear increase in the Fe(A, C) magnetic moment as a function of the number of Fe(B) in the 1nn shell (for $n < 6$) with a rate of $\Delta\mu/\Delta n = 0.34\mu_B$ (Fig. 10). Therefore, the presence of one V atom will decrease the average moment per Fe(A, C) atom to $1.02\mu_B$.

The measured internal field on V impurity (with no V in the 3nn shell) is 47.7 kOe; therefore the $4s$ spin-polarization contribution to the V internal field from a configuration with 8 Fe(A, C) 1nn, 6 Si(D) 2nn 12 Fe(B) 3nn is 47.7 kOe. The hyperfine field shift at a V atom due to the presence of V atoms in the third-near-neighbor shell is composed of the changes in the SP contribution of neighboring Fe(A, C) atoms due to their moment changes, plus the changes in the 3nn contribution due to the V substitution. If one V atom replaces one Fe(B) in the 3nn shell of a V(B), its presence will depress the magnetic moment of 2 Fe(A, C) which are common 1nn to both B atoms (see Fig. 13) by an amount of $0.34\mu_B$ per atom. Thus the average magnetic moment in the 1nn shell of the V atom becomes $0.935\mu_B$ which is 0.92 times the initial value. The first satellite in the V NMR spectrum is shifted to 43.0 kOe, a shift of 0.9 of the initial field value. The close agreement between the relative internal field shift of the first satellite and the moment change produced by 1 V 3nn of another V atom suggests that the main contribution to the internal field change at a V atom arises from the changes in the SP effects produced by the Fe(A, C) moment decrease. For low con-

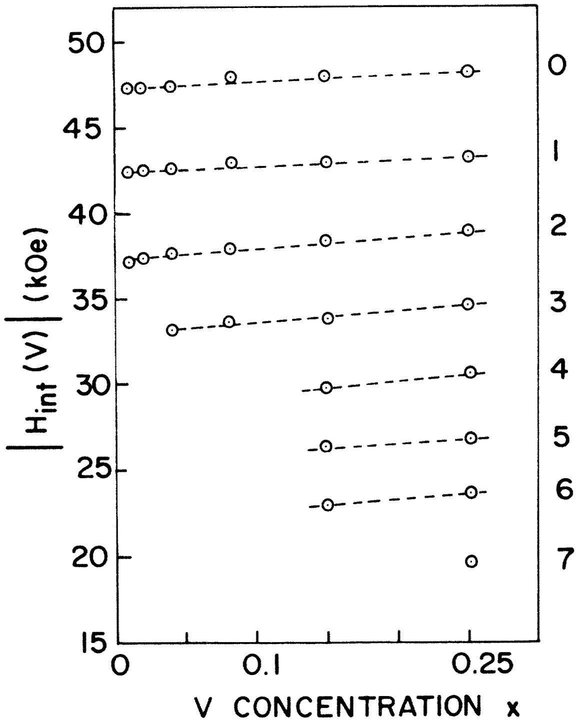

FIG. 14. Concentration dependence of the ^{51}V internal fields. The numbers of 0 to 7 are used to identify the fields of V which have zero to seven 3nn V atoms.

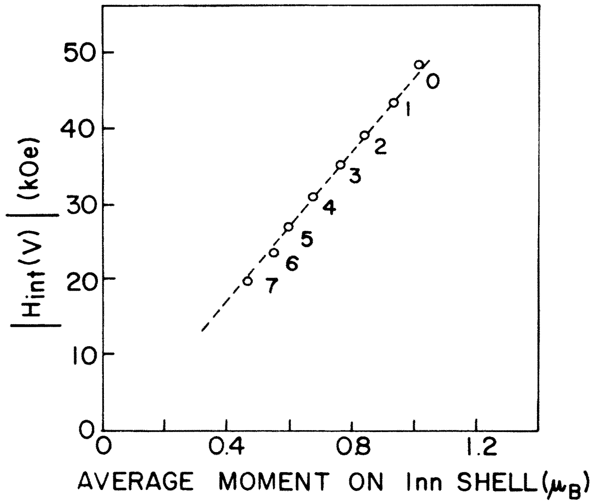

FIG. 15. $|H_{int}(V)|$ corresponding to different satellites vs the average moment on the 1nn shell. The values for the H_{int} are taken for $x=0.25$, where the clearest satellite structure has been observed.

centrations of V, the internal fields corresponding to different satellites in the V spectrum are shown in Fig. 14. For $x=0.25$, seven satellites are clearly resolved. One can notice the tendency for the satellite shifts to decrease with an increasing number of V 3nn and also a slight increase in the field value of the lines with increasing the concentration.

By calculating the average moment changes in the Fe(A, C) 1nn shell of a V atoms due to an increasing number of V 3nn, it is found that the internal field of the corresponding satellites is linearly dependent on the average moment (Fig. 15). The values of the internal fields in Fig. 15 correspond to $x=0.25$, where the clearest satellite structure was observed. The slight change of the positions of the satellites with concentration (Fig. 14) will produce a small change in the slope of the line in Fig. 15 without changing the proportionality between moments and internal fields.

Thus, the presence of V atoms in the 3nn shell of a V perturb the Fe(A, C) 1nn magnetic moments which in turn affect the hyperfine field of V via 4s spin polarization. It should be noted that the extrapolation of the average 1nn shell moment $\langle\mu(A,C)\rangle_{1nn}$ to 0, yields small contribution of opposite sign to the hyperfine field (– 2 to – 3 kOe). This contribution can be attributed to a nonvanishing $(H_{cp}+H_s)$, in other words a very small magnetic moment. It will be shown below that this moment is negative and about $0.02\mu_B$. The slope of the straight line in Fig. 15 gives a change in $H_{int}(V)$ of 49 kOe for a $1\mu_B$ change in the first-near-neighbor shell moment. Therefore, in the first approximation, taking into account only the internal field changes due to the moment perturbations in the 1nn shell, one can write

$$H_{int}(V)=H_{sp}[\langle\mu(A,C)\rangle_{1nn}]+(H_{cp}+H_s)(V), \quad (9)$$

where $(H_{cp}+H_s)(V) \sim -2$kOe.

The first term is related to the 4s spin polarization by the neighboring Fe(A, C) atoms by the formula

$$H_{sp}(V)=A_{4s}(V)p[\langle\mu(A,C)\rangle_{1nn}]n. \quad (10)$$

where $A_{4s}(V)$ is V 4s hyperfine coupling constant, n is the number of 4s electrons involved in the hyperfine coupling, and p the exchange polarization of 4s electrons by the Fe(A, C) 3d magnetic moments. We will use the atomic hyperfine coupling parameters, calculated by Campbell.[24] Accordingly, $A_{4s}(V)=1.11$ MOe/(s-electron). As pointed out by Campbell, these A values are deduced by a interpolation of the atomic hyperfine coupling parameters between those of alkalies and noble metals, and although the absolute values are not expected to describe accurately the coupling in metals, the relative values of A's for elements close to one another in the periodic table are expected to be reasonably correct. We thus find that the polarization of the n s-electrons by an average Fe 3d moment of $1\mu_B$ in the 1nn shell is 44×10^{-3}. The present experiment cannot estimate the number of *s*-electrons involved in the hyperfine interaction, therefore in the internal field calculations for V, Mn, and Fe the product of *np* will be used.

C. Effects of disorder on the V spectra

As shown in the x-ray measurements, V in the Fe_3Si lattice introduces a disorder between the *B* and *D* sites, assuming $(A, C) \leftrightarrow B$ disorder to be small. A simple calculation based on the above model, predicts the changes in the V resonance due to specific configurations. As shown in Table IV, three different possibilities are considered. Indeed, the NMR spectra for $x = 0.02$ and 0.04 (Fig. 8) show a higher-frequency line which could be the combined contribution from the first two cases, while a small peak at ~50.5 MHz could be due to the third. The asymmetry on the low-frequency side of the main line could be the contribution of the second type of disorder to the first satellite. A rough estimation of the degree of $B \leftrightarrow D$ disorder based on the ratio of the areas of the main line and the high-frequency satellite gives an estimate of ~1% disorder, at $x = 0.02$. This value seems reasonable from the systematics point of view (see Fig. 2 and Table II). We wish to point out that, while the x-ray technique is not sensitive enough to detect such a small degree of atomic disorder, the NMR method presently used shows great sensitivity in such a measurement.

The above considerations about $B \leftrightarrow D$ disorder are further supported by studying an off-stoichiometric composition in which excess Fe replaces Si(*D*). Indeed, for the composition $Fe_{3.04}V_{0.04}Si_{0.92}$, the NMR spectrum shows an increase in both the low- and high-frequency contributions to the V resonance (Fig. 16).

D. Effects of high V concentrations

As shown in Fig. 9, increasing V concentrations shift the V internal field to lower values. For the composition Fe_2VSi, the corresponding field is ~12.5 kOe and the resonance is very weak. According to the model adopted above, this field is found at those V nuclei with an average magnetic moment of $0.34\mu_B$ in the 1nn shell which corresponds to a configuration V(*B*) – 8 Fe(*A*, *C*) 1nn, 6 Si(*D*) 2nn, (8 V + 4 Fe)(*B*) 3nn. This configuration, in which there are Fe-Fe 1nn pairs, is possible in Fe_2VSi if one allows for $(A, C) \leftrightarrow B$ disorder. Such a configuration would carry a maximum magnetic moment $1.4\mu_B$/(formula unit) assuming that Fe(*B*) still carries a moment of $2.2\mu_B$. If we further assume that σ_0 for Fe_2VSi (Table II) is due to these ferromagnetic configurations, the fraction of such configurations per formula unit, estimated from the $1.4\mu_B$ moment and the measured value of σ_0, is of the order of 10^{-3}. The ferromagnetic clusters are distributed in Fe_2VSi in which V(*B*) has the neighbor configuration V(*B*) – 8 Fe(*A*, *C*) 1nn, 6 Si(*D*) 2nn, 12 V(*B*) 3nn and in which Fe does not carry a local moment.

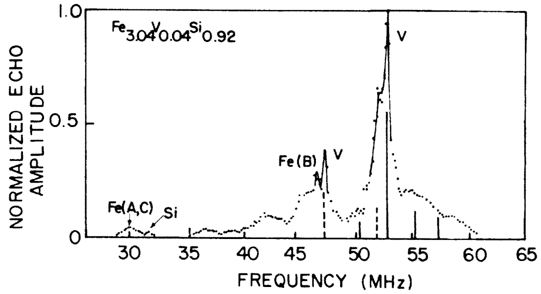

FIG. 16. Spin-echo spectrum for the off-stoichiometric sample $Fe_{3.04}V_{0.04}Si_{0.92}$ at 1.3 K. Inside the spectrum, the solid verticle lines represent the position of the main V line and the lines that originate from the $B \leftrightarrow D$ disorder. The dashed lines represent the position of the 1st satellite and the line due to the disorder. (See text and Table IV.)

The compositions with $x = 0.9$ corresponds to an intermediate state between clusters and long-range magnetic order. This conclusion was reached by analyzing our magnetization data by Arrott plots (σ^2 vs H/σ) at 48, 10, and 3.3 K. Comparison of 48 K with the 10 and 3.3 K curves shows that there is a clear tendency toward ferromagnetic ordering. However, the extrapolation of the straight-line portion of the curves have a positive H/σ intercept at the lowest temperature.

TABLE IV. Changes in the *V* resonance frequency due to three possible changes in the configurations of the first five nn shells surrounding the resonant nucleus. These changes are caused by $B \leftrightarrow D$ disorder. The main resonance is taken at 53 MHz.

Possible disorder	Frequency change	Resonance frequency
1 Fe(*B*) in 5nn shell	1.04	55.1
1 Fe(3nn) ↔ 1 Si(2nn)	1.08	57.2
1 Fe(3nn) ↔ 1 Si(5nn)	0.96	50.7

The peak observed in the plots of $\sigma(H,T)/\sigma(H,0\text{ K})$ vs T around 15 K in low fields (Fig. 6) could correspond to a magnetic transition between the intermediate state and a paramagnetic state.

E. Application of the model to Mn fields in $Fe_{3-x}Mn_xSi$ alloys

A consideration similar to that made for the $Fe_{3-x}V_xSi$ alloys can be employed for the internal field behavior of Mn(B) in the $Fe_{3-x}Mn_xSi$ system. As reported in another paper,[9] the Mn field distribution has a satellite structure similar to that reported here for the V alloys. At low x, Mn atoms substitute in the 3nn shell of another Mn giving rise to neighbor satellites shifted to lower fields by about 5.5 kOe for each Mn 3nn. In Fig. 17, the concentration dependences of the internal fields at these satellites are shown.

The neutron diffraction measurements of the site moment behavior show that in the concentration range $0<x<0.75$ the alloys are ferromagnetic at low temperature and that Mn replaces Fe(B) with roughly the same magnetic moment ($\sim 2.2\mu_B$). Hence we can assume that, in this concentration range, the Mn field shift is due mainly to the changes in the s spin polarization as a result of the Fe(A,C) moment perturbation. The proportionality of the field shifts and the calculated Fe(A,C) moment perturbations holds as is shown in Fig. 18. The s polarization corresponding to the hyperfine coupling constant $A_{4s}(\text{Mn}) = 0.54\text{MOe}/(s\text{-electron})$ is $np = 44\times 10^{-3}$. We wish to point out that the s polarizations, np, at V and Mn produced by the exchange interaction with 1nn Fe moments are equal.

As in V alloys, the two principle contributions to the Mn internal field are

$$H_{\text{int}}(\text{Mn}) = (H_{\text{cp}}+H_s)(\text{Mn}) + H_{\text{sp}}, \qquad (11)$$

where, as before, H_{sp} is proportional to the average moment on the 1nn Fe(A,C) shell with $\Delta H_{\text{sp}}/\Delta\langle\mu(A,C)\rangle_{\text{1nn}} = 67.5\text{ kOe}/\mu_B$. By extrapolating to $\langle\mu(A,C)\rangle_{\text{1nn}} = 0$, we find $(H_{\text{cp}}+H_s)(\text{Mn}) = 192$ kOe and this contribution is due to the local Mn moment. Therefore $H_{\text{sp}} = 68$ kOe and it is produced by the polarization due to Fe(A,C) moments aligned parallel to Mn atoms. H_{sp} has the same sign as the contribution from the Mn local moment. As will be seen, the over-all behavior of the Mn(B) internal fields in $Fe_{3-x}Mn_xSi$ shows the same trends as the Fe(B) field which is known to be negative.[25] Therefore we assign a negative sign to both contributions at the Mn fields. Furthermore, the same assignment can be made for the spin-polarization term in the V internal field.

Now if we assume that Mn, located at the D sites because of $B\rightarrow D$ disorder, has the same moment as Mn(B) but is aligned antiparallel to the Fe(A,C) moments, then the total internal field on the Mn(D) is 192− 68 kOe = 124 kOe. It is to be noted that this value corresponds to the measured Mn NMR signal associated with Mn entering D sites[9] (125 kOe). The ratio of the areas of this signal to that of the main line is about 3%, consistent with the value of the $B\rightarrow D$ disorder measured by x-ray and neutron-diffraction work.[9] The Mn atoms will replace Fe in the 2nn shell of a Mn(D), thus low-

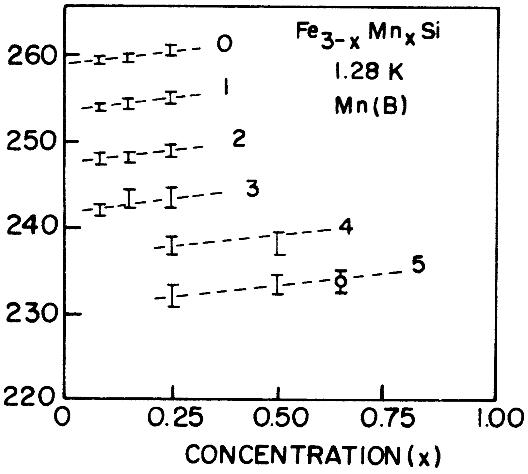

FIG. 17. Concentration dependence of the ^{55}Mn internal field at B sites. The numbers 0 to 5 are used to identify the fields of Mn(B) which have zero to five 3nn Mn atoms.

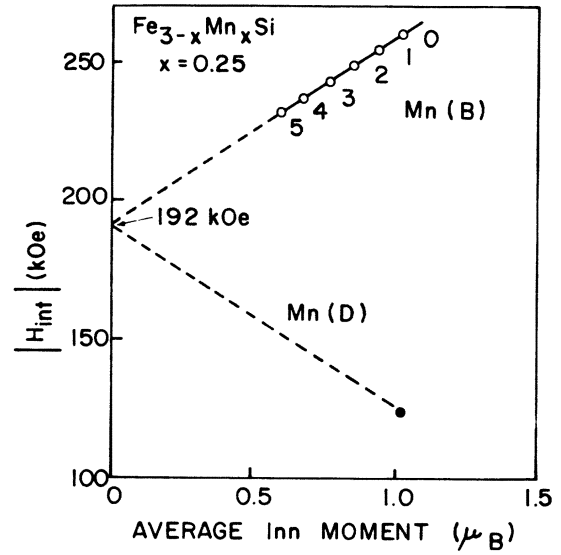

FIG. 18. Upper curve shows $H_{\text{int}}[\text{Mn}(B)]$ in $Fe_{3-x}Mn_xSi$ corresponding to different satellites vs the average moment on the 1nn shell. The internal field values are taken from a $x = 0.25$ alloy (Ref. 9). The lower curve corresponds to the changes in H_{int} for the Mn atoms in D sites due to the $B\longleftrightarrow D$ disorder (see text).

ering the 1nn Fe(*A*, *C*) magnetic moment and reducing the contribution to the Mn(*D*) *s* spin polarization. Without going into more detail of the possible disorder configurations, we wish to mention that for $x = 1$ the frequency of the Mn(*B*) line compared to that of a $x \rightarrow 0$ alloy, is lowered by about 30 MHz, while the Mn(*D*) frequency is increased by the same amount.

The neutron-diffraction results of the moment behavior show that for $x > 0.75$ the average magnetic moment per (*A*, *C*) site remains roughly unchanged up to $x \sim 1.5$ and has a value of $0.4(1)\mu_B$. According to our model, the total SP perturbation produced by the Fe(*A*, *C*) moment change increases the Mn internal field to −214 kOe corresponding to $\langle\mu(A, C)\rangle = 0.34\mu_B$. 214 kOe is the measured Mn internal field corresponding to $x = 1.5$. This fact requires that $(H_{cp} + H_s)$(Mn) is constant throughout this entire concentration range, and thus a constancy of the Mn(*B*) magnetic moment is required by the model. On the other hand, the measured average *B* site moment decreases with increasing Mn concentration between $0.75 < x < 1.75$ as shown in Fig. 12. The magnetic moment data can be understood by assuming a canting of Mn(*B*) moments from the ferromagnetic alignment.

F. Systematics of Fe(*B*) internal field in both $Fe_{3-x}Mn_xSi$ and $Fe_{3-x}V_xSi$ alloys

The Fe(*B*) internal field in Fe_3Si is −337.7 kOe, which is the same value as the field for Fe in Fe metal. The main contributions to this field in the pure metal as calculated by Stearns[26] are −201 kOe from $(H_{cp} + H_s)$ due to the moment on the Fe atom itself and −145 kOe from the conduction-election polarization by the neighboring Fe atoms. The Fe(*B*) magnetic moment in Fe_3Si and the Fe moment in the pure metal are the same. Moreover, substitutions of V or Mn in *B* sites leave the Fe(*B*) moment unchanged at least up to $x = 0.75$. The presence of one V or one Mn in the 3nn shell of a Fe(*B*) atom shifts the Fe internal field by ~7.5 kOe. This shift does not depend on whether the impurity has a local moment or not and it increases in proportion to the number of impurity atoms substituted (Ref. 7). In Fig. 19 the positions of the satellites of Fe(*B*) in $Fe_{3-x}Mn_xSi$ as a function of concentration are plotted. In the system $Fe_{3-x}V_xSi$, the Fe(*B*) satellites could only be resolved at low concentrations of V (Fig. 8) but the similarities in the position and the sign of the shift make us believe that the trend holds true for higher concentrations. The plot of the H_{int}[Fe(*B*)] versus the average moment on the 1nn shell gives a straight line (Fig. 20).

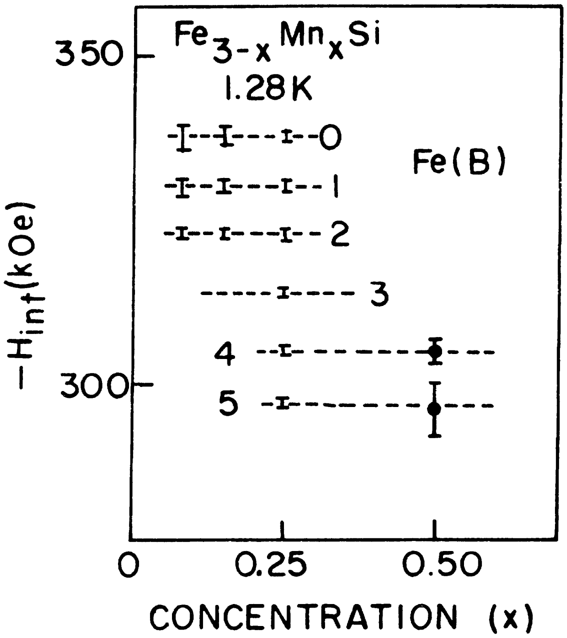

FIG. 19. Concentration dependence of the internal field at the ^{57}Fe nuclei in the *B* sites in $Fe_{3-x}Mn_xSi$. The numbers 0 to 5 are used to identify the fields of Fe(*B*) which have zero to five 3nn Mn atoms.

Assuming that the Fe(*B*) field shifts are produced by changes in the polarization of 4*s*-like electrons due to the magnetic moment perturbations on the Fe(*A*, *C*) surrounding the resonant nuclei, and using for the hyperfine coupling constant A_{4s}(Fe) the value 1.78 MOe/(*s*-electron),[24]

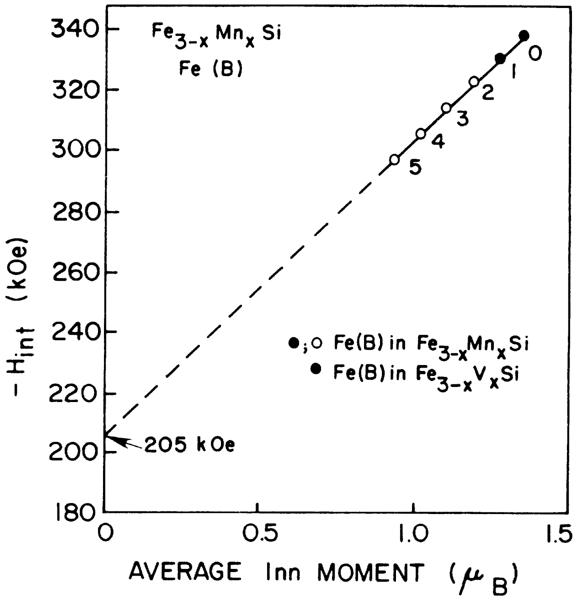

FIG. 20. H_{int}[Fe(*B*)] corresponding to different satellites in $Fe_{3-x}Mn_xSi$ and $Fe_{3-x}V_xSi$ vs average magnetic moment in the 1nn shell. The numbers 0 to 5 indicate the satellites from Fig. 19.

the polarization np at Fe(B) is -56×10^{-3} for V and Mn as impurities in the B site. The extrapolation of the straight line in Fig. 20 to $\langle\mu(A,C)\rangle_{1\mathrm{nn}}=0$ gives the contribution $(H_{\mathrm{cp}}+H_s)$ $=-205$ kOe, in agreement with Stearns's[26] calculated value.

Our results show that the main contribution to the s spin polarization of Fe atoms and implicitly of V and Mn is produced by the exchange coupling between the 4s spins in the vicinity of the resonant nucleus and the Fe magnetic moments from the 1nn shell. This coupling produces a polarization which is essentially the same for V, Mn, and Fe. Therefore the changes in the internal field at the B sites due to substitutions in the 3nn shell are transmitted indirectly via the coupling with 1nn Fe(A,C). As x is increased from 0 to 0.75 the average moment on the 1nn of a B site decreases from 1.35 to ~0.34μ_B but the moments of Fe(B) and Mn(B) are unchanged. From the derived value for $(H_{\mathrm{cp}}+H_s)$ (Fe) $=-205$ kOe corresponding to a moment of 2.2μ_B, one finds that the local moment of Fe(B) contributes -93.18 kOe/μ_B to its internal field. Using the same ratio for Mn(B) and V(B) the calculated values of the moments from the internal field data, $(H_{\mathrm{cp}}+H_s)$ (Mn) $=-192$ kOe and $(H_{\mathrm{cp}}+H_s)$ (V) ~ 2 kOe, are 2.06 and ~0.02μ_B, respectively. Thus calculations using internal field data according to this model give moments which agree with neutron-diffraction[19] and magnetization[10] results.

G. Behavior of the Fe(A,C) internal field in $Fe_{3-x}V_xSi$ and $Fe_{3-x}Mn_xSi$ alloys

The model used to explain our magnetization and internal field data has been based on measurements of the internal fields, magnetization, and magnetic moments of the Fe(A,C) sites in $Fe_{1-c}Si_c$ alloys for $0.227<c<0.26$. The major assumption was that a Fe(A,C) moment depends on the number of Fe(B) 1nn, while the Fe(B) moment does not change in this concentration range.

Our experimental results show that the substitution of V or Mn in Fe_3Si produces a satellite structure at low frequency in the Fe(A,C) spectra (see Fig. 7 of Ref. 9 and our Fig. 8). In the $Fe_{3-x}V_xSi$ system, because of overlap from the V resonance overlap, the first Fe(A,C) satellite could be observed only in the $x=0.04$ sample while in $Fe_{3-x}Mn_xSi$ the structure was resolved up to $x=0.65$. In Fig. 21 we show the positions of the Fe(A,C) satellites for both systems as a function of concentration. The main Fe(A,C) line corresponds to a field of ~-218 kOe, the first satellite is at -180 kOe for Fe(A,C) sites with one Mn in the 1nn shell and at ~-167 kOe for sites with one V in the 1nn shell.

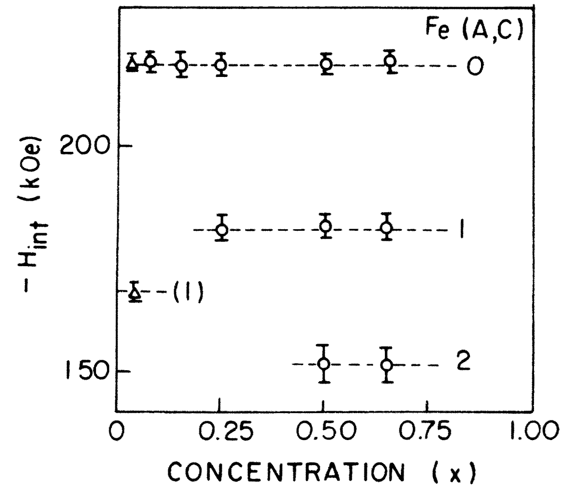

FIG. 21. H_{int}[Fe(A,C)] corresponding to different satellites on $Fe_{3-x}Mn_xSi$ (○) and $Fe_{3-x}V_xSi$ (Δ) vs concentration.

Now, we also assume for Fe(A,C) that $(H_{\mathrm{cp}}+H_s)$ is proportional to its 3d magnetic moment at a rate of -93.18 kOe/μ_B, and calculate this contribution to the internal field at Fe(A,C) atoms for several 1nn configurations (see Table V, column 4). These field values have been used to calculate the SP contributions to the total internal field and the s polarizations which are listed in Table V. It is to be noted that the resulting SP contribution from the 1nn moments, $(H_{\mathrm{int}})_{\mathrm{meas}}-(H_{\mathrm{cp}}+H_s)_{\mathrm{calc}}$, is practically constant for the three configurations in $Fe_{3-x}Mn_xSi$, but decreases for the V substituted alloy. This can be understood by considering that the polarization np is a function of the average 1nn magnetic moment surrounding the Fe(A,C) atom. Indeed, for the $Fe_{3-x}Mn_xSi$ system, Mn atoms replace Fe with approximately the same magnetic moment and, therefore, the average magnetic moment in the 1nn shell of Fe(A,C) does not change while in $Fe_{3-x}V_xSi$, V replaces Fe with a near zero moment, reducing the average 1nn shell moment. The average of the s polarization produced by 1nn moments around Fe(A,C) is ~-50×10^{-3} (Table V, column 6). This value corresponds to a polarization np of $-46(3)\times10^{-3}$ per μ_B. The V substitution reduces the average moment from 1.1 to 0.83 for one 1nn and the calculated np value is $-49(2)$ $\times10^{-3}/\mu_B$.

The similarity of the np values produced by 1nn moments at Fe(A,C) and at Mn, V, and Fe(B) proves that the local spin polarization produced by the exchange coupling between 3d magnetic moments and the 4s spins is proportional to the magnitude of the magnetic moments.

The extensive agreement of the model with ex-

TABLE V. Analysis of various contributions to the hyperfine field at the Fe(A,C) sites.

1nn configuration[a]	μ[Fe(A,C)][b] (μ_B)	H [Fe(A,C)][c] (kOe)	$(H_{cp}+H_s)$ [Fe(A,C)][d] (kOe)	H_{sp}[e] (kOe)	$10^3 np_{tot}$[f]	$\langle\mu\rangle_{1nn}$[g] (μ_B)	$10^3 np$[h]
4Fe 4Si	1.35	217.8(3.0)	125.8	92(3)	51.7(2.0)	1.1	47(2)
3Fe 1Mn 4Si	1.02	181.7(3.0)	95.07	87(3)	48.7(2.0)	1.08	45.1(2.0)
2Fe 2Mn 4Si	0.68	152.6(5.0)	63.4	89(5)	50.1(3.0)	1.07	46.9(3.0)
3Fe 1V 4Si	1.02	168(3)	95.04	73(3)	40.9(2.0)	0.83	49.3(2.0)

[a] 1nn configurations around Fe(A,C) atoms corresponding to the main line and two resolved satellites in $Fe_{3-x}Mn_xSi$, and the main line and one satellite in $Fe_{2.96}V_{0.04}Si$.

[b] The local moments of Fe(A,C) sites from the model for the 1nn configurations listed (Fig. 10).

[c] The measured internal fields on Fe(A,C) atoms (Fig. 21).

[d] Calculated values of $(H_{cp}+H_s)=\mu[\mathrm{Fe}(A,C)]\times 93.18$ kOe$/\mu_B$.

[e] $H_{sp}=(H_{int})_{meas}-(H_{cp}+H_s)_{calc}$.

[f] The total s polarization produced by 1nn shell $np=H_{sp}/A_{4s}(\mathrm{Fe})$ using $A_{4s}(\mathrm{Fe})=1.78$ MOe/(s-electron).

[g] $\langle\mu\rangle_{1nn}$ is the average moment per atom on 1nn shell where $\mu(\mathrm{Fe})=2.2$, $\mu(\mathrm{Mn})=2.06$ and $\mu(\mathrm{V})=-0.02\mu_B$.

[h] 4s local spin polarization produced by $1\mu_B$ in 1nn shell.

periment supports the original assumption that the Fe(A,C) moments depend only on the number of Fe 1nn. Since substitutions of Mn or V for Fe(B) equally reduce the Fe(A,C) moment, it is clear that this moment perturbation depends on the chemical nature of the atoms around Fe(A,C) rather than on their moments.

V. SUMMARY AND CONCLUSIONS

The $Fe_{3-x}T_xSi$ (T = V, Mn) alloys are a model system in which one can test in an unambiguous fashion the effect of local environments on the internal field distributions and the moment behavior. Furthermore, it provides a clear understanding of exchange paths which are of considerable importance in the studies of hyperfine interactions.

We have shown, extending the previous small composition investigations in $Fe_{3-x}V_xSi$, that V continues to enter the Fe_3Si matrix predominantly at the B sites up to $x\approx 1.0$, which is the limit of V solubility, and the $B\to D$ disorder increases with x. Fe_2VSi is a Heusler alloy with the $L2_1$ crystal structure.

The $Fe_{3-x}V_xSi$ alloys are ferromagnetic to around $x\approx 0.9$ with the saturation magnetization decreasing linearly with x. The magnetic moment on V for all compositions is ~0, a calculated value of $-0.02\mu_B$ is obtained from internal field data. The V substitution in the B sites reduces the moments of 1nn Fe(A,C) atoms in a linear fashion from their initial value of $1.35\mu_B$. The moment on Fe(B) atoms, on the other hand, remains constant at $2.2\mu_B$. The magnetic state of a Fe_2VSi alloy can be described by magnetic clusters with a moment of $1.4\mu_B$/formula unit and a density of ~10^{-3}.

The internal field at the V site is due to the exchange polarization of the 4s electrons by the 3d moments in its 1nn shell, i.e., Fe(A,C). The satellite splittings in the V NMR spectra are due to V impurities in the 3nn shell. These 3nn substitutions affect the internal fields at the central atom indirectly by reducing the average moment in the 1nn shell Fe(A,C) which in turn changes the local 4s spin polarization. The calculated SP at the B site is $-44\times 10^{-3}/\mu_B$(1nn).

In $Fe_{3-x}Mn_xSi$, $0\leq x\leq 0.75$, Mn enters the B site with a 3% $B\to D$ disorder and with a local moment of $2.20\mu_B$. This substitution causes a reduction in the Fe(A,C) moment similar to that produced by V(B), demonstrating that Fe(A,C) moment depends on the number of its Fe 1nn. The site selectivity, average moment behavior and the internal field distributions are similar in both $Fe_{3-x}V_xSi$ and $Fe_{3-x}Mn_xSi$ alloys, thus suggesting a common approach to understanding these systems.

A model has been proposed for the quantitative evaluation of the hyperfine field distributions at the transition metal elements in both systems and is based on the following:

TABLE VI. Summary of the contributions to the measured internal field for Fe, V, Mn in various sites calculated according to the model. The values of the magnetic moments are calculated from the internal field data by taking $\mu[\mathrm{Fe}(B)] = 2.2\mu_B$.

Nucleus	1nn configuration	$A_4(Z)$ [a] [MOe/s-electron]	$H_{cp} + H_s$ (kOe)	$10^{+3} np$	μ_{calc} (μ_B)
V(B)	8 Fe(A,C)	1.11	+2	−44	−0.02
Mn(B)	8 Fe(A,C)	1.54	−192	−44	2.06
Fe(B)	8 Fe(A,C)	1.78	−205	−56	2.2
Fe(A,C)	4 (Fe + Mn) 4 Si	1.78		−46(3)	
Fe(A,C)	4 (Fe + V) 4 Si	1.78		−49(2)	

[a] Values taken from Ref. 24.

(i) The V and Mn enter B sites in $\mathrm{Fe}_{3-x}T_x\mathrm{Si}$ with moments of ~0 and ~$2.2\mu_B$, respectively. These moments and that of Fe(B), $2.2\mu_B$, remain constant up to $x = 0.75$.

(ii) The V or Mn in B sites reduce the Fe(A,C) moment which is critically dependent on the number of Fe 1nn.

(iii) The internal fields of atoms at the B and A,C sites are given by the equation

$$H_{\mathrm{int}} = (H_{\mathrm{cp}} + H_s) + H_{\mathrm{sp}} .$$

The first term is proportional to the local moment of the atom while the second one is proportional to the average moment of the 1nn shell.

(iv) The local moments of all atoms contribute to the internal fields at the same rate as Fe, i.e., 93.18 kOe/μ_B, while the 1nn moment contribution to the local 4s spin polarization has an average value of $5 \times 10^{-2}/\mu_B$.

This model has allowed us to view the data on the moments, magnetization and internal fields of these alloys in a coherent and self-consistent fashion, and has made calculations of moments, contribution to the internal field and the 4s polarization possible in $\mathrm{Fe_3Si}$ and its alloys of V and Mn. A summary of these calculations is presented in Table VI.

Thus the model provides a further indication that the interactions in $\mathrm{Fe_3Si}$ and its alloys are short range. Specifically, contributions from the polarization of 4s electrons are due to interactions with moments at the 1nn shell and more distant neighbors contribute to SP by perturbing the 1nn shell moment. Except for these indirect effects, Fe(A,C) seems to screen B atoms from any direct interaction with a more distant neighbor either magnetically or chemically.

Using all of the NMR and magnetization data together with the model, a canting of the Mn moment in $\mathrm{Fe}_{3-x}\mathrm{M}_x\mathrm{Si}$, $0.75 < x < 1.6$, has been predicted. Furthermore, disorder contributions to the NMR spectrum have been identified laying a foundation for the development of a general analytic technique of great precision.

Note added in proof. Recent neutron results [S. Pickart *et al.* (unpublished)] indicate that a $(A,C) \leftrightarrow B$ disorder of about 5% exists in this system. This indicates that both $B \leftrightarrow D$ and $(A,C) \leftrightarrow D$ disorders would be between 0 and approximately 5% over the composition range studied.

ACKNOWLEDGMENTS

The authors wish to thank J. A. Cannon for his assistance with the magnetization measurements, L. V. Azaroff for his interest in the x-ray work, and S. Skalski for several stimulating discussions. We are grateful to Fordham University for the use of their arc melting facilities and A. Corbeil for his technical assistance during the course of this work.

---

†Supported in part by the University of Connecticut Research Foundation.

*Also at Department of Engineering and Applied Sciences, Yale University, New Haven, Conn. 06520.

[1] T. J. Burch, T. Litrenta, and J. I. Budnick, Phys. Rev. Lett. 33, 421 (1974).

[2] T. Litrenta, Ph.D. thesis (Fordham University, 1975) (unpublished).

[3] S. Pickart, T. Litrenta, T. J. Burch, and J. I. Budnick, Phys. Lett. A 53, 321 (1975).

[4] A. C. Switendick, Bull. Am. Phys. Soc. 21, 441 (1976).

[5] C. Blaauw, G. R. Mackay, and W. Leiper, Solid State Commun. 18, 729 (1976).

[6] V. Niculescu, K. Raj, T. J. Burch, and J. I. Budnick,

Bull. Am. Phys. Soc. 20, 586 (1975).

[7] K. Raj, V. Niculescu, J. I. Budnick, and S. Skalski, AIP Conf. Proc. 29, 348 (1976).

[8] K. Raj, V. Niculescu, and J. I. Budnick, Bull. Am. Phys. Soc. 21, 441 (1976).

[9] V. Niculescu, K. Raj, T. J. Burch, and J. I. Budnick, Phys. Rev. B 13, 3167 (1976).

[10] W. A. Hines, A. H. Menotti, J. I. Budnick, T. J. Burch, T. Litrenta, V. Niculescu, and K. Raj, Phys. Rev. B 13, 4060 (1976).

[11] V. Niculescu, T. Litrenta, K. Raj, T. J. Burch, and J. I. Budnick (unpublished).

[12] A. Paoletti and L. Passari, Nuovo Cimento 32, 1450 (1964).

[13] J. I. Budnick, S. Skalski, T. J. Burch, and J. H. Wernick, J. Appl. Phys. 38, 1137 (1967).

[14] See references for Fe-Si phase diagram in M. Hansen, *Constitution of Binary Alloys* (McGraw-Hill, New York, 1958).

[15] R. L. Bergner, V. U. S. Rao, and S. G. Sankar, AIP Conf. Proc. 29, 325 (1976).

[16] G. B. Johnson and E. O. Halle, J. Phys. Chem. Solids 29, 193 (1968).

[17] P. J. Webster, J. Contemp. Phys. 10, 559 (1969).

[18] S. Foner, Rev. Sci. Instrum. 30, 548 (1959).

[19] S. Yoon and J. G. Booth, Phys. Lett. A 48, 381 (1974); J. G. Booth (private communication).

[20] G. Schlatte, G. Inden and W. Pitch, Z. Metallkd. 65, 94 (1974); H. Wever and G. Frohberg, *ibid.* 65, 747 (1974).

[21] M. B. Stearns, Phys. Rev. 129, 1136 (1963).

[22] J. I. Budnick and S. Skalski, in *Hyperfine Interactions*, edited by A. J. Freeman and R. Frankel (Academic, New York, 1967), p. 724.

[23] M. Rubinstein, G. H. Stauss, and J. Sweck, Phys. Rev. Lett. 17, 1001 (1966).

[24] I. A. Campbell, J. Phys. C 2, 1338 (1969).

[25] K. Raj, V. Niculescu, T. J. Burch, J. I. Budnick, and R. Frankel, Proceedings of the Joint Intermag.-MMM Conference, Pittsburgh, Penn., June, 1976 (unpublished).

[26] M. B. Stearns, Phys. Rev. B 4, 4069 (1971); 4, 4081 (1971).